IOSR Journal of Applied Physics (IOSR-JAP)
e-ISSN: 2278-4861.Volume 10, Issue 2 Ver. II (Mar. – Apr. 2018), PP 01-11
www.iosrjournals.org

Study oftheOptical, Morphological andElectrical Properties ofSynthesized Undoped andAl-Doped ZnO Thin Films Nanoparticles via Spray Pyrolysis Technique Deposition

D. O. Samson[1,2*], A. M. Ramalan[1] and J. A. Rabba[3]
[1]*Department of Physics, University of Abuja, P.M.B 117, Abuja, Nigeria.*
[2] *School of Physics, Universiti Sains Malaysia, 11800 USM, Gelugor, Penang, Malaysia.*
[3] *Department of Physics, Federal University, Lokoja, Kogi State, Nigeria.*
Corresponding Author: D. O. Samson

Abstract:*Thin films (TFs) having composition ofundoped and Al-doped ZnO were deposited onto synthesized glass substrates using spray pyrolysis technique with doping concentrations of 0, 10, 15 and 20% at annealing temperature of 200^{o}C - 400^{o}C. The effects of the doping concentrations on the optical properties of the as-deposited films were investigated by exploiting UV-Visible spectrophotometer and Bruker profilometer to evaluate quantify surface roughness and thicknessin the spectra range of 250nm to 1200nm. The obtained results show that metallic Zn films have a preferential (011) c-axis orientation instead of the common (002) predilection. The average transmittance of the undoped film is over 90%, while the doped films have less than 70% mean transmittancein the visible region and the observed optical band gap energy increases from 3.12eV to 3.24eVwith the increase of Al doping concentrations. The lowest resistivity of 248.13Ωcm and the highest conductivity of 403.0 x 10^{-5}(Ωcm)$^{-1}$ was obtained in the film with 20% doping concentrations.*
Keywords: *Spray pyrolysis technique, Band gap, Al doping, ZnO TFs, UV-Vis*

Date of Submission: 10-03-2018 Date of acceptance: 28-03-2018

I. Introduction

A study of the optical, structural, morphological and electrical properties of thin films (TFs)is very vital due to it helps in optimizing films parameters for better device applications. The fascinating physical, chemical and optoelectronic properties of zinc oxide (ZnO) that suits several applications such as spintronic devices, chemical sensors, ultra violet (UV) electronics,laser diode, photovoltaic devices, light emitting diode,gas detector, solar cell technology,piezoelectric devices and most especially as transparent conducting oxide film has make it one of the most promising and multifunctional semiconductor materials[1-2, 5].ZnO has some distinctive advantages over commonly use thin films materials(Cd_2SnO_4 and In_2O_3 etc.) due to its unique combination of appealing properties: stability in hydrogen plasma atmosphere, thermal and chemical stability, non-toxicity, abundance in nature which makes it inexpensive when compared to its competitors, good electrical, optical and piezoelectric behaviours [3]. ZnO exhibits a direct wide band gap of 3.37eV and a relatively high excitonic binding energy of 60MeV at room temperature[4]. It can be doped with a broad variety of ions to meet the demands of various application fields.Among the various dopants, Al has been found to be an efficient n-type dopant for realizing high quantity samples with enhanced band gap energy, higher conductivity, ultraviolet and blue light emission, good optical transmittance and low cost[6]. Al doped ZnO (ZnO:Al)TFs have been prepared with many techniquessuch as electrochemical deposition, pulsed laser deposition [7-8], Rf magnetron sputtering [9], spray pyrolysis [10-11], sol-gel[5, 12-15], chemical-vapor deposition[16], metal-organic chemical-vapor deposition and molecular beam epitaxy [17] etc.Amongstthese techniques, the spray pyrolysis methodwas available and very common due to its simplicity and relatively costeffective, highly adherent, homogeneous, easy control of doping and scalability deposit onto large area substrates.In this present work ZnO:Al TFs were successfully fabricated by spray pyrolysis method with different concentrations and investigate the optical,morphological and electrical properties of the TFs.

II. Experimental Procedure

2.1.Materials

Zinc acetate dehydrate [$Zn(CH_3COO)_2.2H_2O$] (BDH) with ≥ 99.9% purity, Aluminiumchloride[$AlCl_3$] (≥ 99.9% purity) (BDH) and Methyl alcohol (CH_3OH) (BDH)(99.7% purity)were purchased from Quality Control and Testing Laboratories Ltd. Deionized water (DI water) was obtained from an instant purifier with pH

5.5. All other reagents and solvents used for this study were of analytical grade and do not require any further purification.

2.2. Samples Preparation

Substrates (soda lime glass; 0.048cm x 0.028cm) were cleaned ultrasonically with acetone [$(CH_3)_2CO$] and methanolfor 15 minutes and then cleaned with DIwater in order to reduce the deformation of the substrates, after which it was dried in air for about 20 minutes and was then placed on the substrate heater via the substrate holder at a heating rate of $3.5Kmin^{-1}$.Zinc acetate dehydrate solution were weighted and prepared by dissolving 0.02mol (4.39g) of zinc acetate in 100ml of methyl alcoholthat acts as solvent to obtain 0.2M concentration.0.099mol (13.33g) $AlCl_3$ were then dispersed into 100ml of methyl alcoholto produce 0.2M concentration of $AlCl_3$ solution.Theprepared 0.2M precursors containing 10.0, 9.0, 8.5 and 8.0mol of zinc acetate mixture solution and 0.0, 1.0, 1.5 and 2.0mol of $AlCl_3$solutions were added and allowed to dissolve and then used for doping at 0, 10, 15 and 20% of Al doping percentage concentrations. The mixture solutions were manually thoroughly stirred for1 hour 15 minutes to realizing the homogeneity of the composition and the progression of condensation.A syringe pump was then used to feed the precursor mixture solutions through a silicon tubing connected to a small stainless steel needle for atomization. Direct current voltage supply (5-20kV) was applied between the needle tip and the hot substrate plate to get a stable cone-jet mode. The distance between the nozzle and the substrate were kept constant at 8cm for all depositions. The electrostatic spray was then conducted at varying doping at 0, 10, 15 and 20% of Al doping percentage concentration for the four samples during the deposition. The substrate was subsequently heated at 400^oC (752^oF) for 24 hours in airand the spray rate of precursor mixture solutions were retained at 0.05mL/min throughout the experiment. The processes were repeated several times (0, 10, 15, and 20%). After the deposition the deposited films was allowed to cool for 30 minutes at room temperature before characterization. The morphologies of the samples were observed by scanning electron microscopy (SEM) and X-ray diffraction (XRD).

2.2.1. Spectrophotometric Measurements

In order to measure the absorption coefficient and the optical parameters of the thin films as a function of the incident light wavelength, the Axiom Medicals UV 752 spectrophotometer was used to analyse the absorbance data for the prepared thin films at normal incidence of light. The measurements were carried out at 25^oC (77^oF) in the wavelength range of 250nm to 1200nm.

2.3. Surface Characterizations

Thesurface morphology and elemental compositions of the as-synthesized samples powders were characterized by exploiting a Merlin Zeiss scanning electron microscopy (SEM)furnished with an Aztec and INCA microanalysis system with $50mm^2$ silicon drift detector, as well as INCA wavelength dispersive spectrometer (WDS) system as energy dispersive X-ray (EDX) spectrometer. The XRD (D8 Advance Diffractometer, X'Pert' Powder PANALYTICAL Bruker) measurements were executed by the step scanning technique with a monochromatic Cu-K_α($\lambda = 1.54056Å$) radiation. The instrument was operated at 42kV and 40mA with a scan mode of $0.040^o$and constant counting times of 3.17 s/step for 2θ values ranging between 25° and 60°. The electrical characteristics of the films were carried out with a four point probe set-up (QUADPRO-301-6). Bruker profilometer (Veeco Dektak 150 model) was then exploited to evaluate the quantify surface roughness and thickness of the thin films with stylus of 12.5µm, length of 3000µm, resolution of 0.200µm at duration of 50 seconds.

2.4. Determination of Optical Properties

Transmittance describes how much light passes through a sample unchanged. The TFs transmittance (T) and absorbance (A) were computed by using the expression in equation (1):

$$\text{Transmittance}, T = 10^{2-A} \quad (1)$$

$$\text{Absorbance}, A = 2 - log_{10}\,\%T \quad (2)$$

This equationimplies that if all the thin films light is absorbed, then %T will be zero, and absorbance will be infinite but if all the thin films passes through the mixture solution without any absorption, then absorbance will be zero, and %T will be 100%. The optical absorption coefficient (∝)of the glass materials was determined from the Beer-Lambert relation as givenin equation (3):

$$\propto(\lambda) = -ln\left[\frac{1}{T}\right]^{(1/d)} \quad (3)$$

Where, d is the thickness of thin films.The greater attenuation of light in a thin films and higherprobability of raising the electron transfer across the mobility gap with the photon energy represent the higher values of extinction coefficient (k) of light in a medium.

$$n(\lambda) = \frac{[1+R] + [4R - k^2(1-R)^2]^{1/2}}{(1-R)} \quad (4)$$

$$k(\lambda) = \frac{\propto \lambda}{4\pi} \quad (5)$$

Where,$\propto$ is optical absorption coefficient, λ is the wavelength of used X-rays radiation,n is the refractive index, $R$is reflectance and $k$is extinction coefficient of the films.The expression for the optical band gap energy for the as-deposited and annealed thin films were computed from the Tauc's relation [18]by analysing the optical data with the absorption coefficient and photon energy as shown in equation (6):

$$\propto h\upsilon \approx B\left[h\upsilon - E_g\right]^z \quad (6)$$

Where, B is the constant of proportionality which dependence on the electron transition probability, h is the plank's constant, and υ is the frequency of the incident photons,$h\upsilon$ is the energy of the absorbance,E_g is the optical band gap energy, z is a number that determined the type of the optical transition of the gap materials ($z = \frac{1}{2}, \frac{2}{3}$ for allowed direct transitions and $z = 2$ for allowed indirect transitions). The value of optical band gap energy (E_g) is computed by extrapolating the linear graph portion of $(\propto h\upsilon)^2$against photon energy $(h\upsilon)$known as Tauc's plot for the direct optical band gap and have been drawn for thin films deposited with different concentration as illustrated in figure 5, this means that the mode of transition in these films is of a direct nature.

2.5. Determination of Electrical Properties

A QUADPRO-301-6 four point probe was used to determine the sheet resistance and the resistivity of the deposited thin films, after which the conductivity was determine from the resistivity. The sheet resistance$(R_s)$was given by:

$$R_s = 4.53 \times \frac{V}{I} \quad (7)$$

Where, V is the measured voltage between the two inner probes and *I* is the current passed through the outer probes. The resistivity was determined from the relation:

$$\rho = R_s \times d \quad (8)$$

$$\sigma = \frac{J}{E} = \frac{1}{\rho} = \frac{1}{R_s d_c} \quad (9)$$

Where,d_c is the thickness of the conducting layer, $\rho$is the resistivity, σ is the conductivity, J is the current density and E is the electric field.

III. Results And Discussion

3.1.Optical Properties

Film thickness plays an important role in determining the changes that occur in physical properties of metal oxides. The results of the quantify surface roughness and thickness of ZnO:Al thin films as determined by Bruker profilometer (Veeco Dektak 150 model) with stylus of 12.5µm, length of 3000µm, resolution of 0.200µm sample and duration of 50 seconds are presented in figure 1.

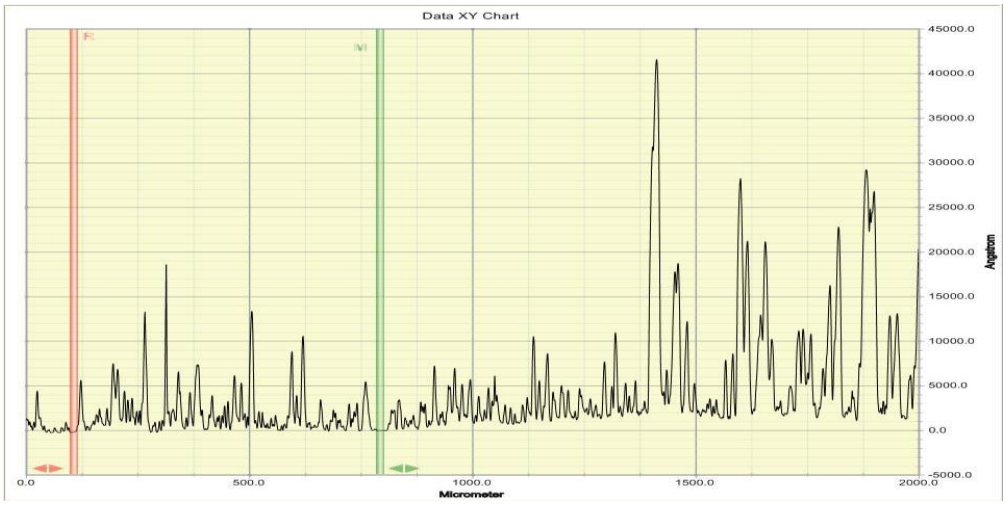

Fig.1: Surface roughness and thickness of Al:ZnO thin films.

The thickness of the Al doped zinc oxide film was found to be 1µm as determined by the Profilometer.

This was used for the determination of absorption coefficient (∝) in order to evaluate the energy bandgap of the material.

3.1.1.Absorbance and Transmittance

Absorbance

The UV-Visible absorption spectra for undoped ZnO and Al doped ZnO thin filmswith doping concentrations labelled as AZO_0, AZO_10, AZO_15 and AZO_20 are shown in figure 2.

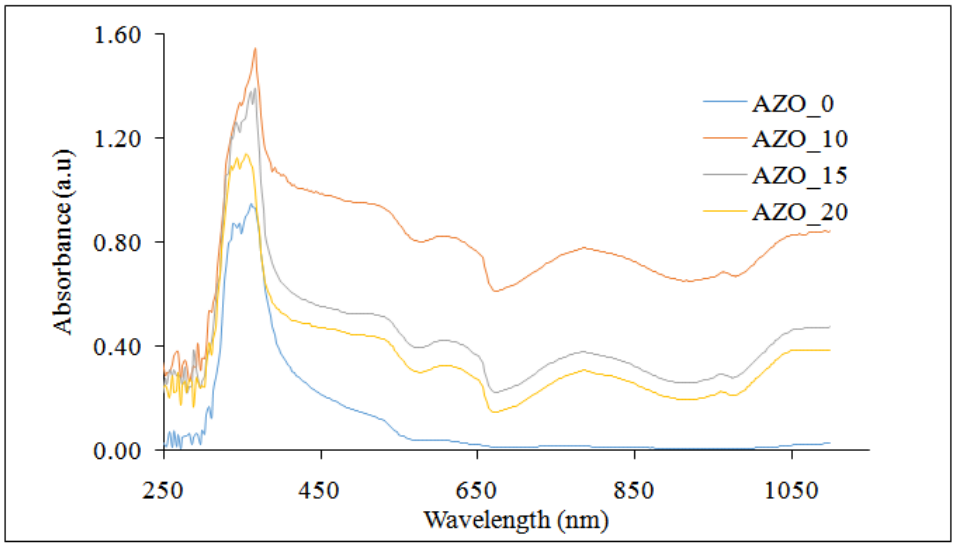

Fig. 2: UV-Visible-NIRwavelength absorption spectra ofundoped and ZnO:Al thin films.

The above figure shows that the absorption edge of the ZnO:Al thin films was observed around 313nm. Sharp absorption peaks were identified around 360nm for all the thin films. There is an observable plateau around 600nm which is absent in the undoped (0%) ZnO thin film, this observation can be ascribed to the presence of Al doping in ZnO materials.A blue shift of the absorption edges can be observed in the doped thin films. Since the higher doping concentration is associated with increase of carrier concentration, the increase of carrier concentration might be helpful to reduce the absorption due to the enlargement of the band gap energy. The absorption intensity increases with the increase on Al doping concentration from 0% to 10 % but then decreases when increasing the concentration to 15% and further decreases with 20%. The decrease exhibited at 15 % and 20 % Al doping may be attributed to enhancement of impurity scattering due to high carrier density beyond the critical value as the carriers might also act as impurity scattering centres.

Transmittance

The UV-Vis transmission spectra of as-synthesised ZnO:Al onto glass substrateswith doping concentrations labelled as AZO_0, AZO_10, AZO_15 and AZO_20 are illustrated in figure 3. This shows that all the films exhibit a strongly marked surface plasmon absorption especially film with (AZO_10)Al doping concentrations.

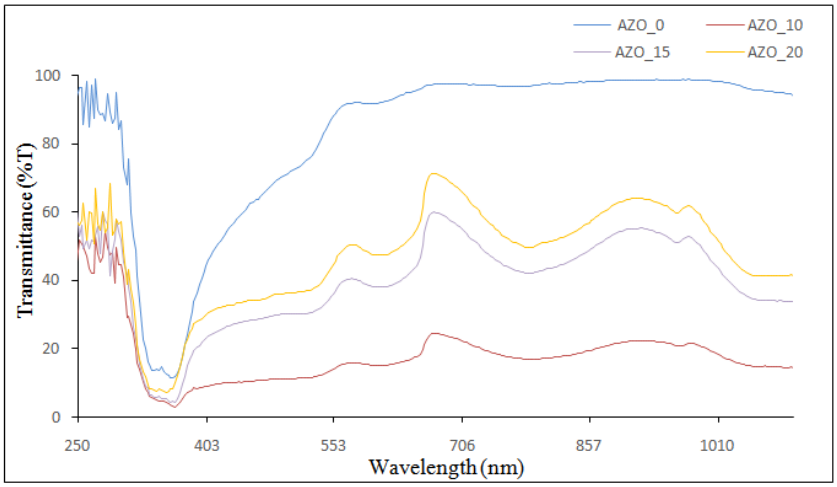

Fig. 3: UV-Visible-NIR wavelength transmittance spectra of undoped and ZnO:Al thin films.

Figure 3 exhibit minimum transmission spectra within the range 333nm to 367nm for all the thin films.The undoped ZnO film have the highest mean transmittance of over 90% in the visible region and showed sharp absorption edges in the UV region, while the doped ZnO:Al films have less than 70% mean transmittance. The doped films had a slightly lower transmittance compared with the undoped films in the visible region [19]. This may be ascribed to the optical scattering caused as a result of the surface morphology and deformation of the crystal lattice. The transmission peaks slightly shifted towards the higher wavelengths as the aluminium concentrations increase as a result of the increases in the films size.

3.1.2.Optical bandgap energy

The optical band gap is defined as the minimum energy needed to excite an electron from the valence band to the conduction band. The optical band for the ZnO:Althin films are shown in figures4 (a-d).

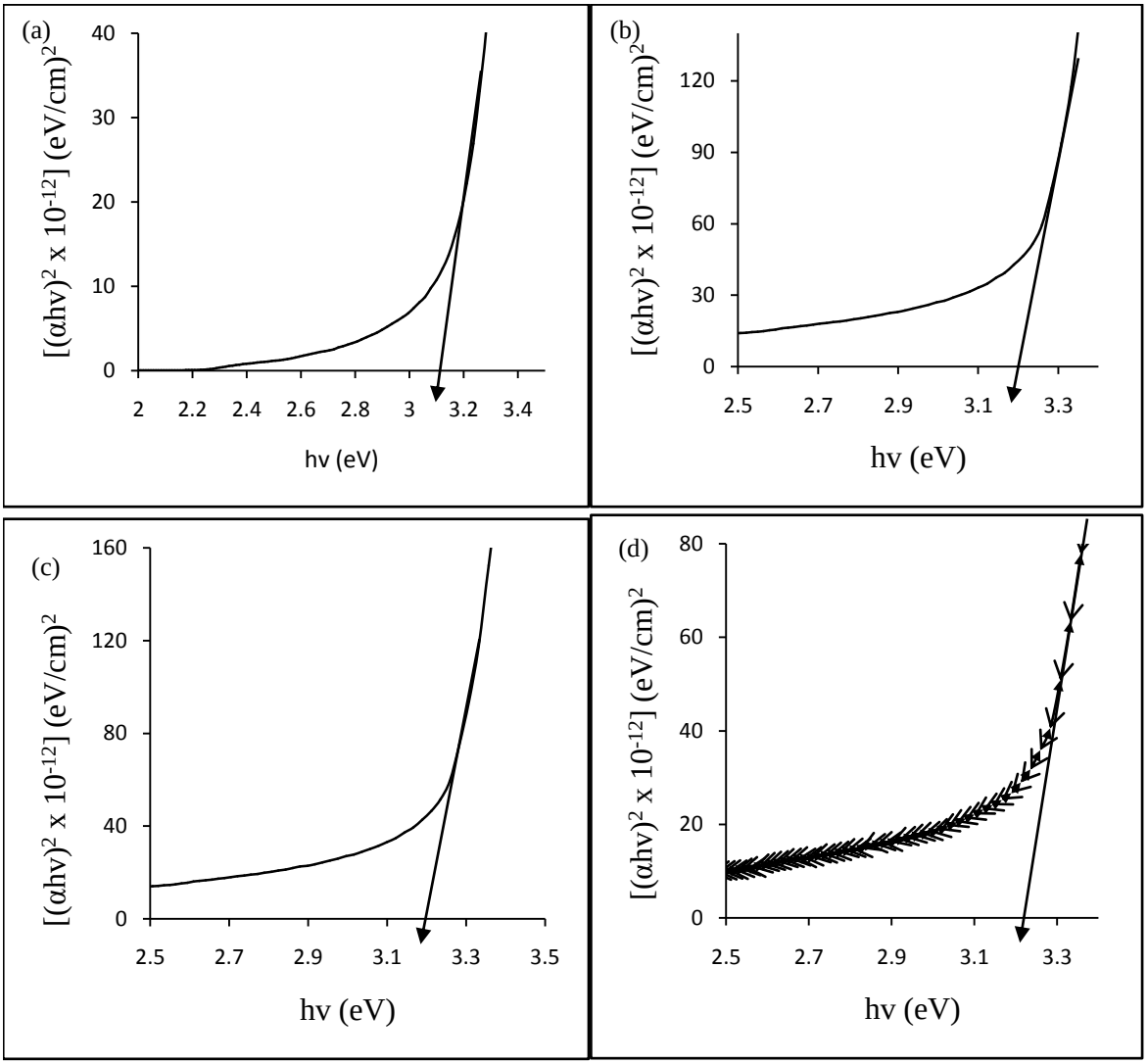

Fig. 4: Tauc plot curves of as-deposited and annealed ofZnO:AlTFs at (a) 0% (b) 10% (c) 15% and (d) 20%.

It was observed from the above figuresthat the optical bandgap energy for the films increases from 3.12eV to 3.24eV as the Al doping concentrations increases after heat treatment.In undoped ZnO thin films the optical band gap equals the energy separation between the band edges, but on doping the donor electrons occupy states at the bottom of the conduction band.The lower value of the undoped films reveals that there is an existence of a high density of defects levels within the band gap measured by the amorphous structure of the ZnO:Al samples. The change in the band gap energy of ZnO:Al films deposited at various doping concentrations can be attributed to two competing phenomena. The first is the Burstein-Moss effect, which shifts positively (widening) the band gap energy to the short wavelength side (blue shift) with an increase in carrier concentration and the other is due to many body effects like the exchange energy due to electron-electron and electron-impurity interactions which occurs when the donor density exceeds a certain value and causes narrowing (red shift) of the band gap energy[20-21]. The increase of band gap energy with increasing annealing temperature may be due to the existence of grain boundaries of the thin films. The atomic structure at the grain boundary is different from that in the grain, which leads to larger free carrier concentrations and existence of potential barriers at the boundaries, leading to the formation of an electronic field and hence an increase of the band gap energy. This increase mighty also be attributed to the partial filling of the conduction band of Al:ZnO thin films resulting in a blocking of the lowest states[22].

3.2. Scanning Electron Microscopy (SEM) Images

The morphological properties of the annealed ZnO:Al TFs was studied by the Zeiss Merlin SEM with an ultra-microtome which uses a focused beam of high energy electrons to generate a variety of signals at the

surface of the films. The samples were gold coated before SEM investigation to study the surface morphology. The analyses of the experimental results obtained from SEM micrograph are illustrated in figures 5(a-d) at different Al contents. The fibers have tendency to decrease in size as the Al content increases as shown by the surface morphology.

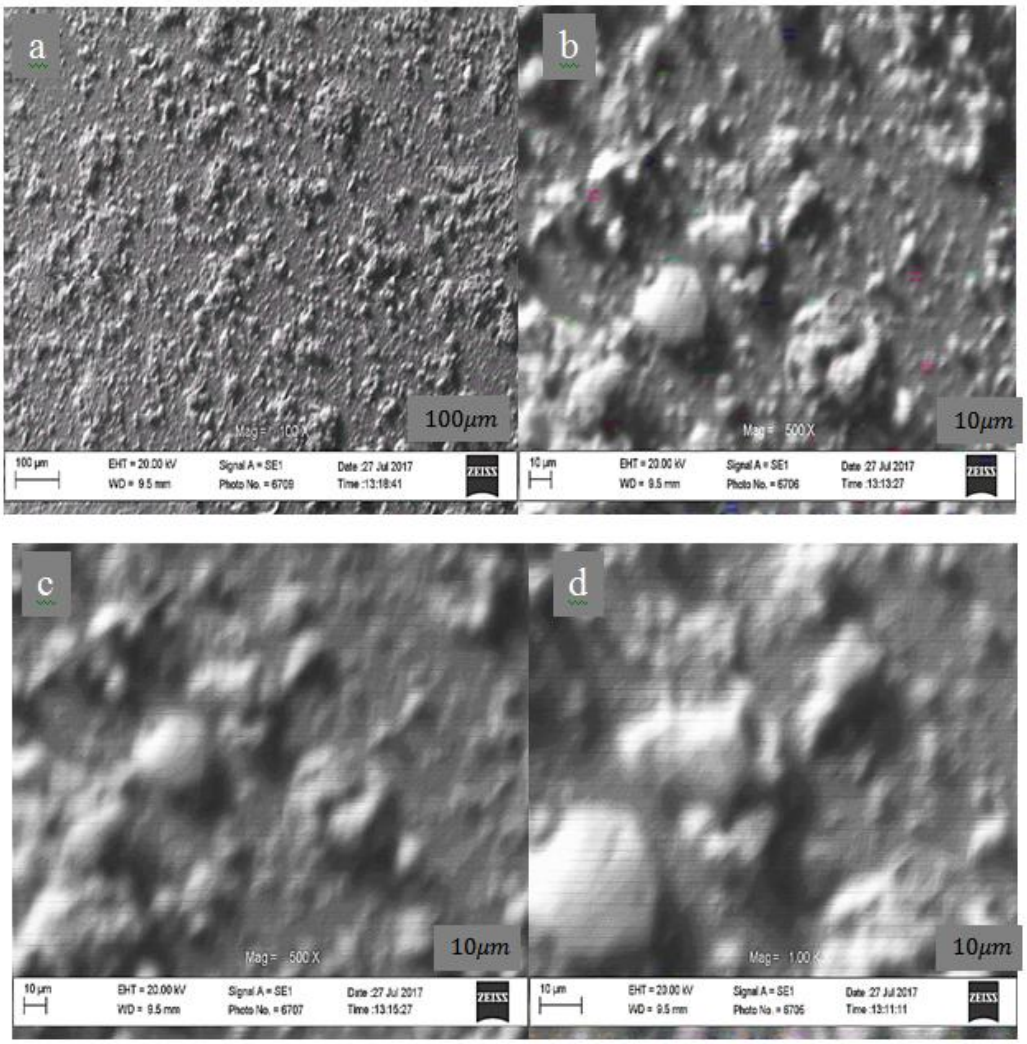

Fig. 5: SEM micrographs images of (a) undoped (b) 10% (c) 15% (d) 20%ZnO:Al.

The SEM images shows that the surface morphology of the films is strongly dependent on the concentration of Al. Uneven surface and dense microstructure are observed in figure 5a for the undoped ZnO films.The particulate grains mostly cover the substrate surface more or less consistently. The surface of the thin films had larger particles as the Al concentrations increased. This revealed that the crystalline phases are embedded in the amorphous matrix for annealed sample at 400^{o}C (752^{o}F) for 24 hours. Thus, the higher annealing temperature seems to have modified the surface morphology of the ZnO:Al TFs. Figure 5(b-d) revealed that the surface showed some cracks, the grain size became denser and larger. The fibers are more densely packed in the films with higher Al contents as the temperature increases which implies that the amount of different form of crystalline phase increase with different crystallized particles sizes. This illustrated that coalescence of particles may have preceded during thermal treatment at higher temperature. It was further observed that the increase in Al contents give rise to a lower porosity and larger average grain size with improved crystalline quality.

3.3. X-ray Diffraction (XRD)

The crystalline phases of thermal oxidation grown ZnO:Al films at elevated substrate temperature of 150^{o}C with various oxidation temperatures of 200^{o}C, 300^{o}C and 400^{o}C were identified in XRD patterns as indicated in figure 6.

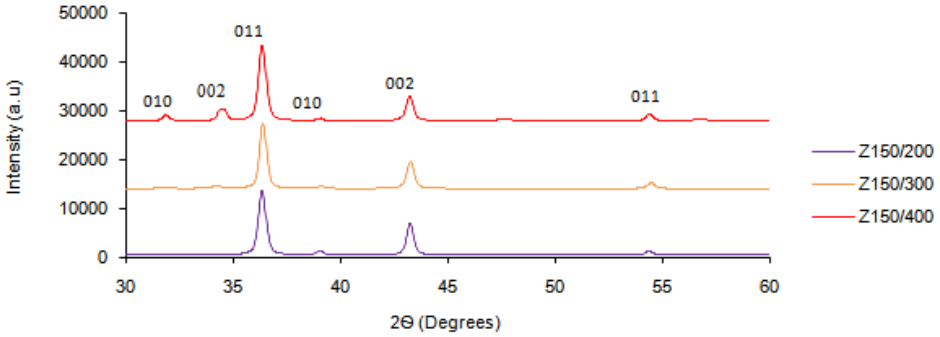

Fig. 6: The XRD patterns of as-synthesizedZnO:Al TFs.

Weobserved a very clear diffraction peaks at 2θ = 32.03°, 34.39°, 36.32°, 39.07°, 43.35° and 54.63° corresponding to (010), (002), (011), (010), (002) and (011) planes. The peak at 2θ = 36.47° with (011) orientation has a strongly marked textured structure of hexagonal ZnO structure, likewise the peaks at 32.23°and 34.55° are indexed to ZnO hexagonal structure [23]. The sharp peaks (010), (002) and (011) planes ascertained at 39.07°, 43.35° and 54.63° are connected with un-oxidised zinc hexagonal system of space group P63/mmc (ICSD: 247158; 52259), this is due to the inadequate flux diffusion of oxygen into the Zn films during the oxidation process as a result of low oxidation temperatures which is lower than 420°C melting point of the Zn films leading. The ZnO films shown a preferentially grown along (011) orientation for all the films instead of the common (002) predilection, which indicated that the growth of ZnO crystallites have preferential (011) plane at low oxidation. This implies that the films grew preferentially in the c-axis orientation. The (010) and (002) ZnO peaks become strongly marked as the oxidation temperatures increased. The lattice parameters 'a' and 'c' values of the prominent peak (011) observed at 2θ = 43.35° are calculated usingequations (10) and (11).

$$a = \sqrt{\frac{1}{3}}c \tag{10}$$

$$c = \frac{\lambda}{\sin\theta} \tag{11}$$

Using the Miller index(hkl) of this(011) plane, the interplanar spacing $(d_{hkl})$for indices (hkl) is evaluated by exploiting the relation in equation (12)[24]. The average crystallite diameter of the oxidised metallic Zn TFs in spherical approximation have been estimated from the Full Width at Half Maximum (FWHM) of more intensive diffraction peaks according to Debye-Scherrer formula [2].

$$d_{hkl} = \frac{1}{\sqrt{\frac{4}{3a^3}[h^2 + k^2 + hk] + \frac{l^2}{c^2}}} \tag{12}$$

$$D = \frac{0.94\lambda}{\beta\cos\theta} \tag{13}$$

Where, λ is the wavelength of used X-rays radiation and $\theta$is the diffraction angle at which the maximum intensity was observed. β is the line broadening at half maximum intensity (FWHM) and D is the particle size.The average lattice strain(ε_{str}) of the ZnO TFs was calculated using the Stokes-Wilson model [25].

$$\varepsilon_{str} = \frac{\beta\cot\theta}{4} \tag{14}$$

The microstructural parameters obtained from the XRD data for the ZnO:Al thin films annealed at different oxidation temperatures are presented in Table 1.

Table 1: Structural characteristics for prominent (011) orientation of the ZnO thin films

Sample	2θ (°)	β (°)	a (Å)	c (Å)	d_{hkl} (Å)	D(nm)	Micro-strain (x 10^{-3})
$Z_{150/200}$	36.87	0.3936	2.81	4.87	2.81	21.27	5.15
$Z_{150/300}$	36.47	0.3540	2.84	4.92	2.84	23.62	4.69
$Z_{150/400}$	36.43	0.3936	2.84	4.93	2.84	21.24	5.22

The table revealed that the lattice constants"c" increased as the annealing temperatures increases while "a" initially increased then remain invariant at 300°C and 400°C. The strain of the thin films at first decreased

when the annealing temperature was increased to 300^{o}C, and as the temperature continued to increase a minimum value of about5.22×10^{-3}nm was obtained.

3.4.Electrical characterization

The effect of doping concentration on the electrical properties of Al doped and undoped ZnO thin films were conferred in Table 2. The relationship between doping concentration and resistivity is shown in figure 7 while figure 8illustratesthe doping concentration and conductivity.

Table 2: Effects of doping concentration on electrical properties of Al:ZnO

Doping concentration (%)	Resistivity ρ (Ωcm)	Conductivity σ x 10^{-5}(Ωcm)$^{-1}$
0	395.26	253.0
10	340.19	294.0
15	331.62	301.5
20	248.13	403.0

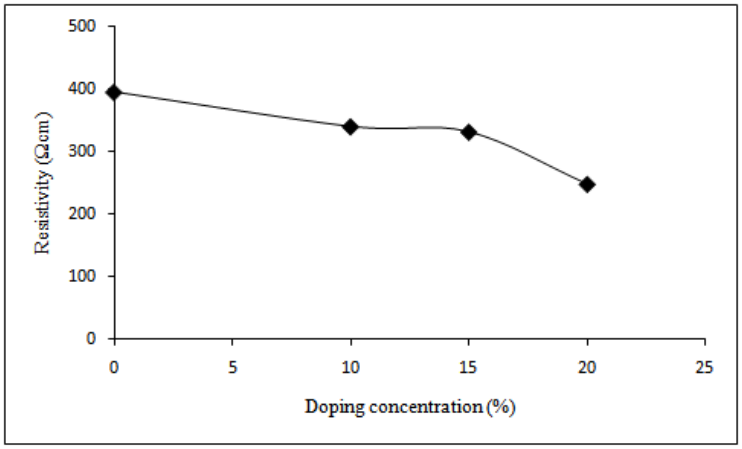

Fig. 7: Variation of resistivity with doping concentration.

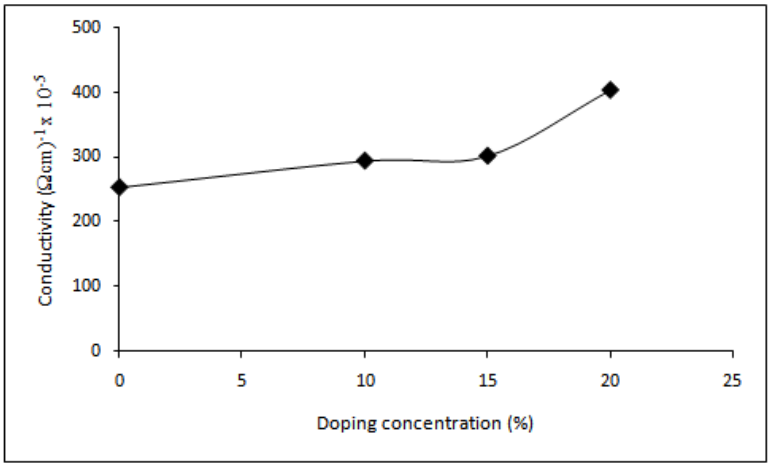

Fig. 8: Variation of conductivity with doping concentration.

According to figure 7, the measured resistivity was found to change with varying in doping concentration in the range of 395.26cmΩ to 248.13cmΩ as the doping concentration increases from 0 to 20% for the thin films.Theobserved decreased in resistivity of the TFs after doping and heat treatment can be attributed to creation of extra free electrons through both Zn substitution by Al atoms and formation of oxygen vacancies during annealing in vacuum atmosphere. This decrease in the resistivity of the TFs compared to ZnO might also be due to the smaller difference in the electronegativity and ionic radius of Al ($r^{3+} = 0.054\ nm$) and Zn ($r^{2+} = 0.074\ nm$), since the dopant element efficiency is a function of its electronegativity as well as the difference between its ionic radius[22]. The radius of Al^{3+} is slightly smaller than that of Zn^{2+}, which lead to a replacement of relatively bigger Zn^{2+} by a smaller Al^{3+} during the formation of the Al doped ZnO TFs. These

replacements lead to a large number of electrons in the doped films, thereby increasing the number of charge carriers and hence increase the conductivity and decrease the resistivity of the doped TFs.

IV. Conclusions

The undoped and Aluminium doped zinc oxide TFs were deposited onto synthesized glass substrates using spray pyrolysis technique at annealing temperature of 200^{o}C - 400^{o}C.The atomic structure at the grain boundary is different from that in the grain, which leads to larger free carrier concentrations and existence of potential barriers at the boundaries, leading to the formation of an electronic field and hence an increase in band gap energy. The films morphological studies revealed that the fibers are more densely packed in the films with higher Al contents as the temperature increases which implies that the amount of different form of crystalline phase increase with different crystallized particles sizes. The films shown a preferentially grown along (011) orientation instead of the common (002) predilection, which indicated that the growth of ZnO crystallites have preferential (011) plane at low oxidation.The average transmittance of the undoped film is over 90%, while the doped films have less than 70% mean transmittance in the visible region and the observed optical band gap energy increases from 3.12eV to 3.24eVwith the increase of Al doping concentrations.It was further observed that the increase in Al contents give rise to a lower porosity and larger average grain size with improved crystalline quality.

Acknowledgements

The authors wish to appreciate the Laboratory staff of the Physics Advanced Laboratory, Sheda Science and Technology Complex (SHESTCO), Abuja, Nigeria for synthesis of the samples and the Microelectronics and Nanotechnology Shamsuddin Research Centre (MiNT-SRC) of theUniversiti Tun Hussein Onn, Malaysiafor SEM and XRD characterization.

Conflict of interest

The authors declare that they have no conflict of interest.

References

[1]. Jagadish, C., Pearton, S. (2006). Zinc Oxide Bulk, Thin Films and Nanostructures: Processing, Properties, and Applications, *Oxford, UK: Elsevier Ltd*.

[2]. Isah, K.U., Ramalan, A.M., Ahmadu, U., Ibrahim, S.O., Yabagi, J.Y., Jolayemi, B.J. (2016). Effect of Zn Film Substrate Temperature on Optical, Structural and Vibrational Characteristics of Thermally Oxidized Zn Films. *Asian Journal of Applied Sciences*. Vol. 9, No. 4, pp. 159-169.

[3]. Tewari, S., Bhattacharjee, A. (2010). Structural, electrical and optical studies on spray deposited Aluminium-doped ZnO thin films. *Pramana-Journal of Physics*, 76(1), pp. 153-163.

[4]. Fan, J., Sreekanth, K., Xie, Z., Chang, S., Rao, K. (2013). *P-type ZnO materials: theory, growth, properties and devices, Prog. Mater. Sci.* 58: 874-985.

[5]. Samia, T., Eiji, Y., Hideyuki, O., Keiichi, N.I. (2016). Electrical stability of Al-doped ZnO transparent electrode prepared by sol-gel method. *Applied Surface Science*. 377:355-360.

[6]. Deng, X.R., Deng, H., Wei, M., Chen, J.J. (2012). Preparation of highly transparent conductive Al-doped ZnO thin films and annealing effects on properties. *J Mater Sci Mater Electron.* 23:413-7.

[7]. Agura, H., Okinaka, H., Hoki, S., Aoki, T., Suzuki, A., Matsushita, T., Okuda, M. (2005). Low-resistive and transparent AZO films prepared by PLD in magnetic field. *Electr. Eng. In Japan*. 151: 40-45.

[8]. Agura, H., Suzuki A., Matsushite, T., Aoki T., Okuda, M. (2003). Low resistivity transparent conducting Al-doped ZnO film prepared by pulsed laser deposition. *Thin solid films*. Vol. 445(2), pp. 263-267.

[9]. Carcia, P.F., McLean, R.S., Reilly, M.H., Nunes Jr. G. (2003). Transparent ZnO thin-film transistor fabricated by rf magnetron sputtering. *Appl. Phys. Lett.* Vol. 82, Issue 7, pp. 1117-1119.

[10]. Bedia, A., Bediaa, F.Z., Aillerie, M., Maloufi, N., Benyoucef, B. (2015). Morphological and Optical properties of ZnO thin films prepared by spray pyrolysis on glass substrates at various temperatures for integration in solar cell. *Energy Procedia*. Vol. 74, pp. 529-538.

[11]. Rakhesh, V., Vaidyan, V.K. (2009). Effect of Substrate Temperature and post deposited annealing on the electrical and photoluminescence characteristics of Zinc Oxide films deposited by spray pyrolysis. J. Optoelectronics and Biomedical Mater. Vol. 1, Issue 3, pp. 281-290.

[12]. Jun, M., Park, S., Koh, J. (2012). Comparative studies of Al doped ZnO and Ga doped ZnO transparent conducting oxide thin films. *Nanoscale Research Letters*, 7:639-644.

[13]. Mahroug, A., Boudjadar, S., Hamrit, S., Guerbous, L. (2014). Structural, optical and photocurrent properties of undoped and Al-doped ZnO thin films deposited by sol–gel spin coating technique. *Materials Letters.* 134: 248-251.

[14]. Xu, L., Kaimeng, P., Weibo, L., Dan, H., Shuyang, L., Yude, W. (2014). Optical and gas sensing properties of Al-doped ZnO transparent conducting films prepared by sol-gel method under different heat treatments. *Ceramics International* 40: 9931-9939.

[15]. Saleh, W.R., Saeed, N.M., Twej' W.A., Alwan, M. (2012). Synthesis Sol-Gel Derived Highly Transparent ZnO Thin Films for Optoelectronic Applications. *Advances in Materials Physics and Chemistry*. Vol. 2, No. 1, pp. 11-16.

[16]. Maruyama, T., Shionoya, J. (1992). Zinc oxide thin films prepared by chemical vapour deposition from zinc acetate. *J. Mater. Sci. Lett*. 11: 170-172.

[17]. Wang, J., Cao, J., Fang, B., Lu, P., Deng, S., Wang, H. (2005). Synthesis and characterization of multiple flower-like and ZnO layers on a plane sapphire substrate grown by molecular beam epitaxy. *Journal of crystal Growth*. 538: 237-239.

[18]. Patil, S., Shinde, S., Rajpure, K. (2012). Physical properties of spray deposited Ni doped zinc oxide thin film s, *Ceram. Int.* 39:3901-3907.

[19]. Pan, Z., Tian, X., Wu, S., Yu, X., Li, Z., Deng, J., Xiao, C., Hu, G., Wei, Z. (2013). Investigation of structural, optical and electronic properties in Al–Sn co-doped ZnO thin films, *Appl. Surf. Sci.* 265: 870-877.
[20]. Sharma, N., Kumar, R. (2014). Effect of substrate temperature on structural and Optical properties of thermally evaporated thin films of F16CuPc. *Advances in Applied science Research.* 5(2), pp. 111-116.
[21]. Shan, F.K., Yu, Y.S. (2004). Band gap energy of pure and Al-doped ZnO thin films. *J Eur Ceram Soc*. 24:1869-72.
[22]. Thomas, D. O. (2015). Electrostatic Spray Deposited ZnO:Al Thin Film: The Role of Substrate Temperature. M.Sc Thesis, Federal University of Technology, Minna, Nigeria.
[23]. Isah, K.U., Ramalan, A.M., Jolayemi, B.J. (2016). Structural, Morphological and Optical Characteristics of Low Temperature Oxidized Metallic Zinc Films. *British Journal of Applied Science and Technology.* Vol. 16, No. 6, pp. 1-9.
[24]. Al-Hamdani, N.A., Al-Alawy, R.D., Hassan, S.J. (2014). Effect of Gamma Irradiation on the Structural and Optical Properties of ZnO Thin Films. *IOSR Journal of Computer Engineering.* Vol. 16, No. 1, pp. 11-16.
[25]. Thool, G.S., Singh, A.K., Singh, R.S., Gupta, A., Susan, A.H. (2014). Facile synthesis of flat crystal ZnO thin films by solution growth method: A micro-structural investigation. *Journal of Saudi Chemical Society*. Vol. 18, pp. 712-721.

D. O. Samson "Study Of The Optical, Morphological And Electrical Properties Of Synthesized Undoped And Al-Doped ZnO Thin Films Nanoparticles Via Spray Pyrolysis Technique Deposition." IOSR Journal of Applied Physics (IOSR-JAP), vol. 10, no. 2, 2018, pp. 01-11.